On The Complexity Of A Social Behavior Model

Christoforos Somarakis
Institute For Systems Research
University Of Maryland, College Park
csomarak@umd.edu
John S. Baras
Institute For Systems Research
University Of Maryland, College Park
baras@umd.edu

In this paper, we discuss a social behavior model in cellular automata. This model came as a result of research in dynamical structures of networks as these were constructed out of game theory and statistical physics. We define it a dynamical system on the planar grid and study it's behavior by varying it's parameters under different initial configurations.

1 Introduction

Cellular automata are perhaps the simplest mathematical representations of complex dynamical systems and networks. They are spatially and temporally discrete, deterministic models characterized by local interaction and an inherently parallel form of evolution. Although the history of cellular can be traced back to 1948, with the work of *J. L. von Neumann* [5], the widespread popularization of these systems was achieved in the 1980s through the work of *S. Wolfram*. Based on computer experiments, he gave a full classification of cellular automata as mathematical models for self-organising statistical systems (collected papers in [11]) that can get related to all scientific fields.
In this paper, we will introduce a new model (we shall call it the $\mathcal{F}$-*rule*) which came as a result of comprehensive research in dynamical structures of networks

Figure 1: The $r = 1$ neighbourhood of the state spaces, outlined with the rectangular sketches. (b)The 2-D space. Every site is defined to interact with each of it's eight neighbors.

...	...	...	...	...
...	(i-1, j-1)	(i-1,j)	(i-1,j+1)	...
...	(i,j-1)	(i,j)	(i,j+1)	...
...	(i-1,j-1)	(i+1,j)	(i+1,j+1)	...
...	...	...	...	...

as these were constructed out of game theory and statistical physics. The $\mathcal{F}$-rule is an outgrowth of the *Prisoner's Dilemma* game [6]. A detailed numerical investigation on a Game Theory perspective of this model was first done in [9]. Here, the model is redefined as a cellular automaton whose dynamics are discussed. It is implemented on the plane and initiates from simple or disordered initial configurations. It's behaviour is observed and classified as some of it's parameters vary. Thorough analysis and discussion, on the amount of complexity this automaton produces in space and time, is carried out. Some preliminary results of this approach are presented in [2].

1.1 Notations and Definitions

The State Space We define a Euclidean space $\mathcal{L} : \mathbb{N}^d$, where $\mathbb{N}$ is the set of natural numbers, as the discrete state space. This is the lattice of d-dimensional sites upon which the automata live, and their dynamics unfold. Every individual site can be defined by a $(1 \times d)$ vector $\mathbf{x}$. Here the $d = 2$ case is considered.

Neighbourhood of a cell Let us now define the regime of the local interactions. Every cell changes it's state after communicating with it's neighbouring cells. We note by $\mathcal{N}(\mathbf{x}, r)$ the range-r neighbourhood of $\mathbf{x}$,without $\mathbf{x}$ itself, and by $\underline{\mathcal{N}}(\mathbf{x}, r)$ the range-r neighbourhood, including $\mathbf{x}$, i.e.

$$\mathcal{N}(\mathbf{x}, r) = \{\mathbf{y} \in \mathcal{L} : 0 < ||\mathbf{x} - \mathbf{y}||_\infty < r\} \tag{1}$$

$$\underline{\mathcal{N}}(\mathbf{x}, r) = \{\mathbf{y} \in \mathcal{L} : 0 \leq ||\mathbf{x} - \mathbf{y}||_\infty < r\} \tag{2}$$

where $||\cdot||_\infty : \mathbb{N}^d \to \mathbb{N}$ is the infinity norm. $r = 1$ means that the neighbourhood of a given centre site $\mathbf{x}$, is the set of sites which are immediately adjacent to $\mathbf{x}$ (see Fig. 1). This is called the *Moore's scheme* [12].

Local Value Space Each cell $\mathbf{x} \in \mathcal{L}$ can assume a finite number of distinct values:

$$\sigma(\mathbf{x}; t) \in \Sigma = \{0, 1, 2, ..., k-1\} \times \mathbb{N} \tag{3}$$

where $\sigma(\mathbf{x}; t)$ is the value of $\mathbf{x}$ at time $t \in \mathbb{N}$. In our paper, we set $k = 2$. The set of states at time t can be either $\sigma = 0$ or $\sigma = 1$. Here, a *black-colored* site means a site in 0 state, and a *white-colored* site is in state 1.

Boundary Conditions Various types of boundary conditions have been proposed in the literature (see [11], [3]).Here we consider exclusively *periodic* boundaries.

Initial Conditions Two types of initial configurations are considered. The *simple seeds*. The system starts from a pattern full of cells at state 1 (white) except one single cell that is in state 0 (black). The growth of cellular automata from such setup should provide models for a variety of physical and other phenomena, such as symmetric growths like crystal or snow-flake growth [11],[7]. The *random seeds*. The system starts from a disordered configuration where each cell is at state 1 or 0 with equal probability $p = 1/2$. This setup reflects the notion of arbitrary initial conditions as it is known in the dynamical system theory and helps us observe the model's self-organization properties as well as the collective behaviour of cells.

Behavioural Classes Different initial configurations give rise to patterns which differ in the details of their appearance the gross overall characteristics of a given pattern appear unchanged: each particular automaton rule yields its own unique recognizable space-time pattern. It is generally believed that all automata rules evolving from disordered initial states fall into one of the following four basic qualitative behavioural classes [11]:

c1 : All sites eventually attain the same value.

c2 : Simple stable states or periodic and separated structures emerge.

c3 : Chaotic, non-periodic patterns are generated.

c4 : Complex, localized propagating structures are formed.

In our simulations, the model appears to exhibit class **c1**, **c2** and **c3** behaviour. Class **c4** was not observed.

The $\mathcal{F}$-Rule The update rule is defined as follows: To each $\mathbf{x} \in \mathcal{L}$, we assign a cost function $V(\mathbf{x}, \mathcal{N}(\mathbf{x}); t) : \Sigma^2 \times \mathbb{N} \to W = \{a, b, c, d\} \subset \mathbb{R}$ such that:

$$V(\mathbf{x}, \mathbf{y}; t) = \begin{cases} a & \text{if } \sigma(\mathbf{x}; t) = \sigma(\mathbf{y}; t) = 0 \\ b & \text{if } \sigma(\mathbf{x}; t) = 0, \sigma(\mathbf{y}; t) = 1 \\ c & \text{if } \sigma(\mathbf{x}; t) = 1, \sigma(\mathbf{y}; t) = 0 \\ d & \text{if } \sigma(\mathbf{x}; t) = \sigma(\mathbf{y}; t) = 1 \end{cases} \tag{4}$$

These costs reflect the tension of local interactions between individual cells. So, the initial step of our rule is that for a fixed value $\sigma(\mathbf{x}; t)$ and for every $\sigma(\mathbf{y}; t)$ of $\mathbf{y} \in \mathcal{N}(\mathbf{x})$ we adjust a number $w \in W$ to $\mathbf{x}$. Finally, for a fixed arrangement

of states in $\mathcal{N}(\mathbf{x})$, site $\mathbf{x}$ receives an overall cost:

$$\begin{aligned}\mathcal{V}(\mathbf{x};t) &= \sum_{\mathbf{y}\in\mathcal{N}(\mathbf{x})} V(\mathbf{x},\mathbf{y};t) \\ &= (1-\sigma(\mathbf{x};t))\Bigg\{\sum_{\mathbf{y}\in\mathcal{N}(\mathbf{x})}\Big[a(1-\sigma(\mathbf{y};t))+b\sigma(\mathbf{y};t)\Big]\Bigg\} \\ &+ \sigma(\mathbf{x};t)\Bigg\{\sum_{\mathbf{y}\in\mathcal{N}(\mathbf{x})}\Big[c(1-\sigma(\mathbf{y};t))+d\sigma(\mathbf{y};t)\Big]\Bigg\}\end{aligned} \tag{5}$$

Finally, $\forall \mathbf{x}\in\mathcal{L}, \mathbf{z}\in\underline{\mathcal{N}}(\mathbf{x})$ the update rule is defined to be:

$$\sigma(\mathbf{x};t+1)=\mathcal{F}(\sigma(\mathbf{z};t))=\sigma(\mathbf{z};t)\text{s.t.}\left\{\mathbf{z}\in\underline{\mathcal{N}}(\mathbf{x}),\ \mathcal{V}(\mathbf{z};t)=\max_{\mathbf{z}\in\underline{\mathcal{N}}(\mathbf{x})}\Big\{\mathcal{V}(\mathbf{z};t)\Big\}\right\}$$

In case there are more than one neighbours with same maximum $\mathcal{V}$ but in different state we avoid the conflict by setting $\mathbf{x}$ to 'follow' the white neighbour. We note by $\mathcal{F}_{(a,b,c,d)}$ the $\mathcal{F}-rule$ for fixed parameters.

Properties and Remarks It can be easily shown that the rule is invariant under additivity, positive multiplication. It also invariant under the inverse of opposite costs, i.e $\mathcal{F}_{(a,b,c,d)}\equiv\mathcal{L}_1\oplus_2\mathcal{F}_{(d,c,b,a)}$. As for the nature of the model, the $\mathcal{F}$-rule is completely deterministic. The a and d costs reflect the local interaction among cells in the same state (we will call them *equal-state* costs), while the b and c costs reflect the local interaction among cells with opposite states (*cross-state* costs). In fact, the local interactions are within a range $r=2$ rather than $r=1$. The decision of $\sigma(\mathbf{x};t+1)$ depends on the values of $\mathcal{V}(\mathbf{z}\in\underline{\mathcal{N}}(\mathbf{x});t)$, but every cost $\mathcal{V}$ is, a result of local interaction between the neighbours of the centre site and their own neighbours. An analytical approach for solving this model is extremely difficult. For this reason, the rule is simulated and every possible combination of the pay-off parameters a,b,c and d is examined. In the simple seed initial conditions we will work as follows: At first, we assume $a<d$. Then additivity invariance implies that we can only consider positive values of the parameters. Additionally, from the multiplication invariance also implies that we can set $a=0$, $d=1$ and let $b,\ c$ free. Similarly, then we consider the $a>d$ Varying the cross-interaction parameters we will see how differently the system behaves and how, for some critical values, the system alters from "regular" to "irregular" behaviour. In the random set-ups we will work in a similar manner.

2 The 2-d $\mathcal{F}$-rule

2.1 Evolution from Simple Seeds

Given the initial setup, the evolution of our automaton depends on the relative values of the b and c parameters as they were set by the $\mathcal{V}$-costs. We moves on

from [2] to further examine the effect of these pay-off values. In that preliminary paper, we took a few analytical steps in order to sketch the mechanism of the rule as a function of the pay-offs. Only the case $a < d$ was examined and led to a phase-transition diagram among regular and irregular patterns. Here together with $a > d$ we also examine the case $a < d$. For the simple-seed setup, nine different schemes are identified (Figs. 2,3):

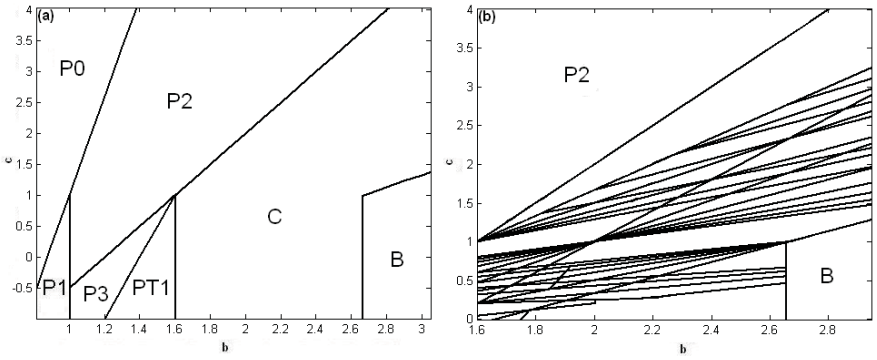

Figure 2: The case $a = 0, d = 1$. (a)A parameter window of the (b, c)-plane, were we have sketched a rough phase transition. While regions **P0**,**P1**,**PT1**,**P2**,**P3** and **B** show regular dynamics, region **C** is rich in irregular behavior. (b)The phase transition focused on the **C** region ($1.6 < b < 2.9$). See text for explanation. The linear boundaries were numerically estimated. The calculation's precision is 10^{-3}.

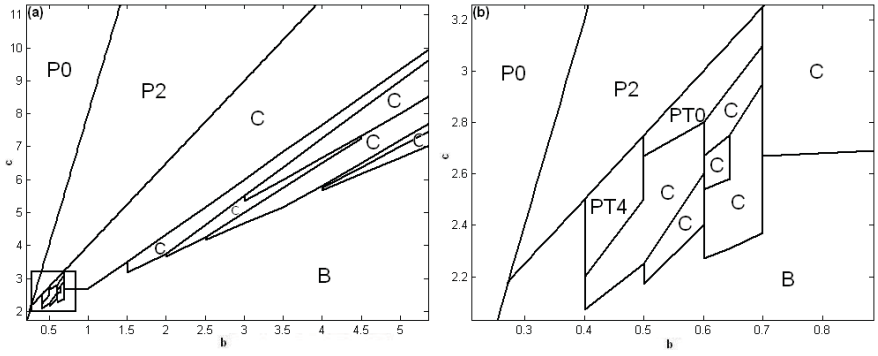

Figure 3: The case $a = 1, d = 0$. (a)A window of the $(b - c)$ parameter subspace as it is numerically calculated. (b) Here a magnification of the rectangular area of Fig. 4(a). All regions have been assigned to a symbol characterizing the generated patterns. See text for more.

P0 : The system *directly* (i.e. without transient states) evolves to homogeneous state where all cells attain the same value (i.e. $\sigma = 1$).

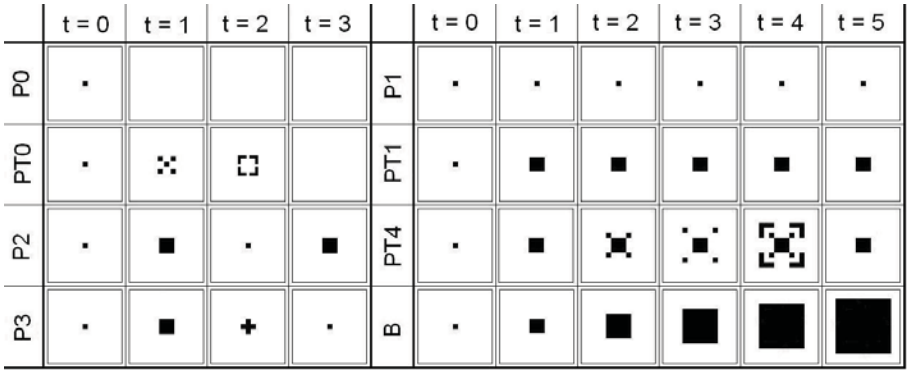

Figure 4: Patterns of regular behavior of the $\mathcal{F}$-rule. When $a < d$, **P0**, **P1**, **PT1**, **P2**, **P3** and **B** appear, while in $a > d$ **P0**, **PT0**, **P2**, **PT4** and **B** appear.

PT0 : The system, after two transient steps, evolves to the homogeneous state $\sigma = 1$

P1 : The system directly evolves to periodic behavior of period 1.

PT1 : The system expands in the first iteration and remains static ever after.

P2 : The system directly evolves to periodic behavior of period 2.

P3 : The system directly evolves to periodic behavior of period 3.

PT4 : The system, after a transient behavior, evolves to period 4.

C : The system exhibits an irregular complex behavior.

B : The systems grows uniformly. At each time step, a regular patter with a fixed density of zero sites is produced.

In Fig. 3(a), we present a raw phase transition pattern on the (b, c) plane for $a < d$ and in Fig. 3(b) a window of the region denoted by **C** (see below for more). The phase-transition diagram when $a > d$ is sketched in Fig. 4. Moving along the diagrams' boundary lines we deal with the set of critical (bifurcation) values. For instance, in Fig. 3(a) at the **PT1**, **C** boundary we step on the critical vertical line of $b = 8/5$. Similarly, the **C** to **B** boundary consists of the connected lines $b = 8/3$ and $c = b - 5/3$ [2]. It is obvious that **P0**, **PT0**, and **B** belong to the **c1** class, **P1**, **PT1**, **P2**, **P3**, **PT4** are in **c2** and **C** is of **c3** type.

2.2 The C region

Contrary to the other sections, **C** is a parameter subspace, where the automaton appears to exhibit extraordinary dynamics. The $\mathcal{F}$-rule in this region generates only expanding patterns. In Fig. 4 we put a few of these patterns with snapshots of their evolution is presented. Every sub-figure contains the plane pattern

as well as a space time evolution of the lattice's main diagonal (the line that includes the initial black cell). Unlike the other regions, these carpets have no simple faceted form and in most cases non-uniform interior. Additionally, due to symmetric initial states, they are invariant under all the rotation and reflection symmetry transformations. In order to identify part of the **C** dynamics, we implemented various techniques that we present below. We numerically estimated the transition phase space for $a < d$ (The $a > d$ case is discussed in [2]).

Global dynamics on a fixed lattice $\mathcal{L}$ We keep the lattice size constant ($N = 50$) with periodic boundaries and explore the system's long term behaviour. Each simulation test was run for at most $20,000$ iterations. The dynamic behaviour is, classified in three qualitative families:

$\mathcal{C}_1$ After a transient behaviour, all sites of $\mathcal{L}$ attain the same value. A class similar to **PT0** type but with much longer and more complicated transient time. The patterns begin to expand until their frontiers meet.

$\mathcal{C}_2$ After a transient behaviour, all sites of $\mathcal{L}$, converge to strictly periodic (period-$T > 1$) motion. By *strictly periodic of period* T we mean that $\exists\, T, T' \in \mathbb{N} :\ \sigma(\mathbf{x}; t) = \sigma(\mathbf{x}; t + T)\ \forall\ \mathbf{x} \in \mathcal{L}, t \geq T'$. The difference from $\mathcal{C}_1$ is, obviously, in the system's final state.

$\mathcal{C}_3$ The dynamic evolution does not converge to any of the previous two classes. A typical class $\mathcal{C}_3$ behaviour is the one that after a sufficiently large number of iterations ($= 20,000$) the pattern neither, strictly, repeats itself, nor turns out to a homogeneous state.

2.3 Complexity

In this section, we will discuss the complexity of our model. The cost parameters belong to **C** classes. The system initiates from a simple-seed configuration and evolves on a large size matrix $\mathcal{L}$.

Growth Dimensions The limiting structure of patterns generated by the growth of cellular automata from simple seeds can be characterized by various *growth dimensions*. The type of dimension we will make use of depends on the *boundary* of the pattern. The boundary may be defined as the set of sites that can be reached by some path on the lattice that begins at infinity and does not cross any non-zero sites. This set of limiting cells can thus be found by a simple recursive procedure:

$$D_g = \lim_{t \to \infty} \frac{log(\#_0(t))}{\log(t)} \tag{6}$$

where $\#_0(t)$ is the number of black cells generated at time t. In general, growth dimensions describe the logarithmic asymptotic scaling of the total sizes of patterns with their linear dimensions. Since the limit may not exist, one

defines the upper and lower spatial growth dimensions D_g^+, D_g^- in terms of the upper and lower limits of (6), respectively. In Fig. 5 we present $log - log$ plots of some rules: In case (a) where we have dendritic boundary growth (see Fig. 4(a)) $D_g = 1.98 \pm 0.01$. In case (b) (Fig. 4(b)) there is both non-uniform interior and boundary evolution and we have $D_g = 2.1 \pm 0.02$. In case (c) (Fig. 4(e)) the expanding pattern creates non-uniform interior while the boundaries remain faceted and $D = 1.9 \pm 0.01$. Finally, in case (d) (Fig. 4(d)) $\log \#_0(t)$ varies irregularly with $\log(t)$ the most; there $D_g^+ = 2, D_g^- = 0$. We also note that almost all **C**-type rules follow one of the four growth curves presented in Fig. 5.

Space-Time Patterns A direct technique for examining the asymptotic behavior of cellular automata is through a state subspace analysis. One may choose to define Poincaré-like sections and study the dynamic evolution of this subspace. We chose the diagonal of the two-dimensional lattice with time (as in Fig. 4). The reason this specific section is selected is that it is the axis of symmetry along which the system expands more rapidly than any other direction. One might also consider the main horizontal axis [2]. Moreover, we surely prefer to deal with one-dimensional patterns since such automata are, more effectively, handled. In Figs. 4(a)-(e) we present examples of space-time sections which reflect the dynamics of the 2D $\mathcal{F}$-rule in a one-dimensional projection. Of course, Eq. (6) can also be applied here: (a) $D_g = 1$, (b) $D_g^+ = 0.947 \pm 0.002$, $D_g^- = 0.8629 \pm 0.001$ (c) $D_g = 0.99 \pm 0.01$ (d) $D_g = 1.161 \pm 0.003$ (it is noted here that the space-time section is the *Sierpinski gasket*, a self-similar object with $D_{fractal} = \log 3 / \log 2 \backsimeq 1.58$). The **C**-region generates patterns of complex behavior typical members of the **c3**-class as the non-integer values of the growth dimensions suggest.

3 Evolution from Random Seeds

Completely disordered setups are members of the set of all possible configurations. Patterns generated from them are thus typical of those obtained with any initial state. The presence of structure in these patterns is an indication of self-organization on the lattice [12]. Consider the average fraction of white cells defined as $\rho(t) = \frac{\#_1(t)}{\#_0(t)+\#_1(t)} = \frac{\#_1(t)}{N^2}$ where $\#_i(t)$ is the number of cells that are at state i at time t. Qualitatively speaking, three types of collective behavior are identified.

Equal-State costs greater than Cross-State costs $(\mathbf{a,d} > \mathbf{b,c})$ In this case, the evolution favors the interaction among cells with the same states. The final state of the system is a static equilibrium where the occurring pattern is an assembly of black and white "ghettos" as in Fig. 6(a). We see there that the system starts from the, completely disordered, state at $t = 0$. The system reaches the equilibrium within the first seven time steps. The last diagram presents index $\rho(t)$ (see figure comments for more). If we increase one of the two

leading parameters, say a, we will observe the increase of the black sites over white. In fact, for $a > a_c = 8/7$ all sites attain the same (black) state. The same holds, of course, if we turn d over a. The role of b, c parameters, as long as they do not exceed a and b, is that of controlling the average number of black and white cells respectively. For such non-zero values of the intermediate costs we have the critical inequality $7a + b > 8d$ instead of a_c.

Cross-State costs greater than Equal-State costs $(\mathbf{b,c > a,d})$. Completely different patterns occur when "cross-state" costs b, c are larger than "equal-state" costs a, d. The typical code for this family is $\mathcal{F}_{(0,1,1,0)}$ a simulation of which is presented in Fig. 6(b). The system after a transient mode of 65 time steps, settles down to a period-10 cycle. One may notice the black and white regions inside of which there are white and black kernels, respectively. They are these cellular kernels that, actually, motivate this oscillation. In general, an $\mathcal{F}_{(a,b,c,d)}$ where $b, c > a, d$ generates orbits that after a transient time converge to periodic attractors. The transient time, the period of the attractor and the *magnitude of oscillation* $\rho(t)/(1 - \rho(t))$ are random quantities (they depend on the initial state). What we are only sure of, is that the system will converge to even-period limit sets. The role of a, d costs is, as long as they remain lower than cross-state costs, similar to the first family. They merely stabilize the mean amount of black and white cells respectively, in other words, the mean value of ρ in steady state.

One Equal-State parameter is between the Cross-State parameters. $(\mathbf{d < b < a < c})$ The last case is studied by fixing $d = 0, b = 0.5, c = 1$ and vary a. We then increased parameter a from $a = 0$. The moment a jumps over b a new type of behavior appears. In particular, for:

(a) $0 < a < b = 1/2$. The system behaves like in the previous case since we have $b, c > a, d$. The attractors are of even period and the mean value of $\rho(t)$ is around 0.63.

(b) $1/2 < a < 2/3$. The system does not converge. Here a typical rule is $\mathcal{F}_{(0.5001,0.5,1,0)}$ which we present in Fig. 6(c) and study ever after. Like in the case of simple seeds we have simulated the model for about $20,000$ iterations. The system neither converges to a static equilibrium nor to a periodic circle. This "aperiodic" evolution in a deterministic model like ours resembles chaos. In the following, we will further support this idea.

(c) $2/3 < a < c = 1$. The system converges to periodic attractors.

(d) $a > 1$. All sites attain the zero state.

Stability An important tool to characterize the evolution of an automaton, is the discrete *Green function*. We can get a glimpse of the form of the Green functions for a selected rule by plotting the *difference pattern*. These are pattern

of difference between two evolutions of the same rule starting from two different initial states. The rate of growth of these patterns is defined to be

$$\Delta(n) = \mathcal{F}^n[\sigma(G_1; 0)] \oplus \mathcal{F}^n[\sigma(G_2; 0)] \tag{7}$$

This rate gives an idea of the speed with which various features in a cellular automaton evolution may propagate through the lattice. The information we are interested in, is the small perturbation in the initial setup. The asymptotic rate is a number analogous to the *Lyapunov exponents* in the dynamical systems theory. (for a consistent approach see [8]). In this work, two random setups that differ in one site are generated. We let them run under the same $\mathcal{F}$-rule and used (7) to see the resulting effect. We used three different rules; one of each category. The results are presented in Fig. 7. In Fig. 7(a) there is the simulation result of $\mathcal{F}_{(1,0,0,1)}$. The initial perturbation was directly either eliminated or stabilized to a plastic difference like in Fig 7(a). This dynamic behavior signifies of the system's expected robustness in initial perturbations. So in (a) $\mathcal{F}_{(1,0,0,1)}$, any noticeable difference will not expand for long and will remain plastic for all times. In (b) $\mathcal{F}_{(0,1,1,0)}$. In this case the initial difference expands during the transient steps. As soon as the patterns converge to periodic attractors, the difference pattern will converge too. Hence the range of the effect is expected to be a function of transient length. Global instability is reported for the family of §IV**C** rules. In Fig. 7(c) we present the difference pattern of $\mathcal{F}_{(0.5001,0.5,1,0)}$. In this category a single site perturbation is enough to lead to two totally different orbits (see 11(c),(iv) and (v)) which, nevertheless, evolve with the same $\overline{\rho}$. From space time sections we observe the linear growing difference which implies exponential divergence (asymptotic in case of infinite lattice) of nearby configurations [3],[12], i.e. chaos.

4 Discussion and Concluding Remarks

In this paper, we introduced a cellular automaton model capable of exhibiting multifarious dynamic behavior. We examined the model using two types of initial configurations, two space dimensions and two space topologies, as well. In each case, we valued it's cost parameters and attempted to shed light upon different aspects of the model's dynamics by classifying the collective and asymptotic behavior of the emerging patterns. In this work we have adopted the Moore's interacting scheme but be assured that with another scheme, new phase transition properties will take place. We then tested the model with disordered initial setups and explored the collective behavior. The three types of behavior reported are: A coarsening evolution that leads to labyrinthine patterns. The second type is this of the system's convergence to periodic cycles and is characterized by strong self-organization. The system starts from an arbitrary initial state and follows a finite transient time and settles down to periodicity. Moreover, the system seems to have limited sensitivity to initial conditions only during the transient mode. This phenomenon is known in the dynamical system theory

as *transient chaos* [**?**]. The last case we met is this when one equal-state cost (a) gets in the middle of the cross-state costs (b, c with $b < c$). The result is a structurally unstable system which behaves aperiodically and is characterized by sensitivity to small perturbations. Regarding the deterministic nature of our model we have every reason to believe that this is a chaotic behaviour.

Growth Inhibition So far, we have thoroughly discussed the 2-D model's transition from smooth to complex behaviour. We have an idea of what happens but still do not know why this happens. Complex patterns occur is because of the Growth Inhibition phenomenon. This is very common in the way some crystals grow as well as in many physical and biological systems [12],[10]. At a microscopic level the crystallization occurs when a liquid or gas is cooled below its freezing point. The procedure always start from an individual seed and unfolds by adding more frozen atoms to their surface. In some cases, whenever a piece of ice is added to the snowflake, there is some heat which is released averting the addition of further pieces in the vicinity. So, instantly, freezing is allowed at some directions while it is inhibited at the rest. This effect can be simulated by a cellular automaton that updates cells to black if they have exactly one black neighbor and white if they have more than one black neighbor.

A deterministic Ising Model There are striking similarities of the $\mathcal{F}$-rule evolving from random seeds and the *Ising Model* from Statistical Physics [4]. In that model there is the same grid of cells and at each global configuration of the cell's states (up/down spins), an energy is assigned as a function of the cell's neighbors state. Finally a probability measure is defined for the global state space and three classes of collective behavior are identified. The *ferromagnetic* case where the interaction tends to keep neighboring spins aligned the same; the *antiferromagnetic* where the system tends to reinforce pairs in which the spins are of opposite orientation, and the *noninteracting* case. Varying some system parameter's the Ising Model goes through these three phase transitions similarly to the transitions reported here. In fact, the ferromagnetic case is similar to the coarsening evolution that leads to labyrinthine patterns (Eq. (12)). This is what the family of $\mathcal{F}_{(1,b<1,c<1,1)}$ rules generates and is represented by Fig. 7(a). The antiferromagnetic case is similar to $\mathcal{F}_{(a<1,1,1,d<1)}$ presented in Fig. 7(b). The noninteracting case bears a resemblance to $\mathcal{F}_{(1/2<a<2/3,0.5,1,0)}$ (Fig. 7(c)).

Applications If we consider $\mathcal{L}$ to be a compact society of citizens (cells), then white, $\sigma = 1$, state would adjust to a *good* man while the black, $\sigma = 0$, would adjust to the *bad* man. Our lattice is, thus, a collection of concrete neighborhoods which interact, according to a cost function (eq. (6) or Fig. 2(a)). So suppose that $\mathbf{x}$ is a good man with s also good neighbors and $(8 - s)$ bad neighbors. Then, for every good $\mathbf{y} \in \mathcal{N}(\mathbf{x})$, $\mathbf{x}$ gains a reward of d units while for every bad, our hero may get a penalty of c units. Variations of the rule could be a good models for simulating the market interaction. Economics is a subject of social networks, in which the procedure of learning or imitation

and then reply among interacting individuals is fundamental (a game theory approach can be found in [1]). In $\mathcal{F}$-realm, sites would be sellers and buyers. To make this more intriguing one could raise the number of possible states and then separates them in two categories: people who sell certain goods, and of people who buy them. Cost values would form the relative value between goods. Although strictly deterministic, the $\mathcal{F}$-rule produces patterns that bear great resemblance to stochastic models. It may have applications in physical (statistical mechanics - lattice gas theory) [4] or biological (interaction between malignant and non-malignant cells) networks as well as in computer networks. However, further research on this model is required.

Bibliography

[1] Cartwright, E., "Imitation, coordination and the emergence of nash equilibrium", *Int. J. Game Theory* **36** (2007), 116–135.

[2] C.E Somarakis, G.P. Papavassilopoulos, and F.E. Udwadia, "A dynamic rule in cellular automata.", *22nd European Conference on Modelling and Simulation*, (2008), 164–170.

[3] Ilachinski, A., *Cellular Automata. A Discreet Universe*, World Scientific NJ (2002).

[4] Kindermann, J., and J.L. Snell, *Markov Random Fields and Their Applications*, AMS NY (1980).

[5] Neumann, J. Von, "The general and logical theory of automata.", *Celebral Mechanisms in Behavior - The Hixon Symposium* (1948), 1–41.

[6] Nowak, A.M., and R.M. May, "Evolutionary games and spatial chaos.", *Nature* **359** (1992), 826–829.

[7] Packard, N., "Cellular automaton models for dendritic crystal growth.", *Institute for Advanced Study* (1985), (preprint).

[8] Shereshevsky, M. A., "Lyapunov exponents for one-dimensional cellular automata", *J. Nonlinear Sci.* **2** (1992), 1–8.

[9] Wiederien, R.J., and F.E. Udwadia, "Global patterns from local interactions.", *Int. J. Bifurcation and Chaos* **14**, 8 (2004), 2555–2578.

[10] Willson, S., "On convergence of configurations", *Discrete Math.* **23** (1978), 279.

[11] Wolfram, S., *Automata and Complexity. Collected Papers*, Addison-Wesley (2000).

[12] Wolfram, S., and N.H. Packard, "Two-dimensional cellular automata", *J. Stat. Phys.* **38** (1985), 901–946.

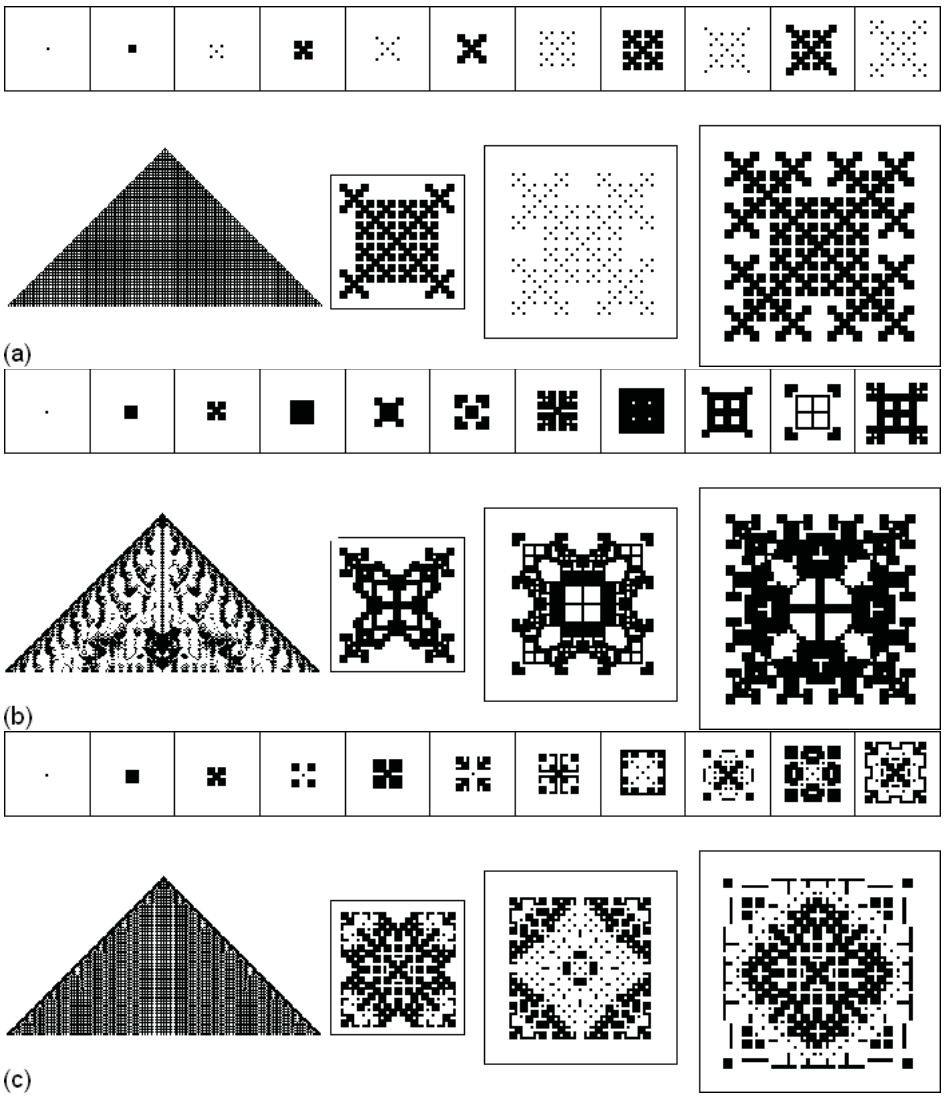
(a)
(b)
(c)

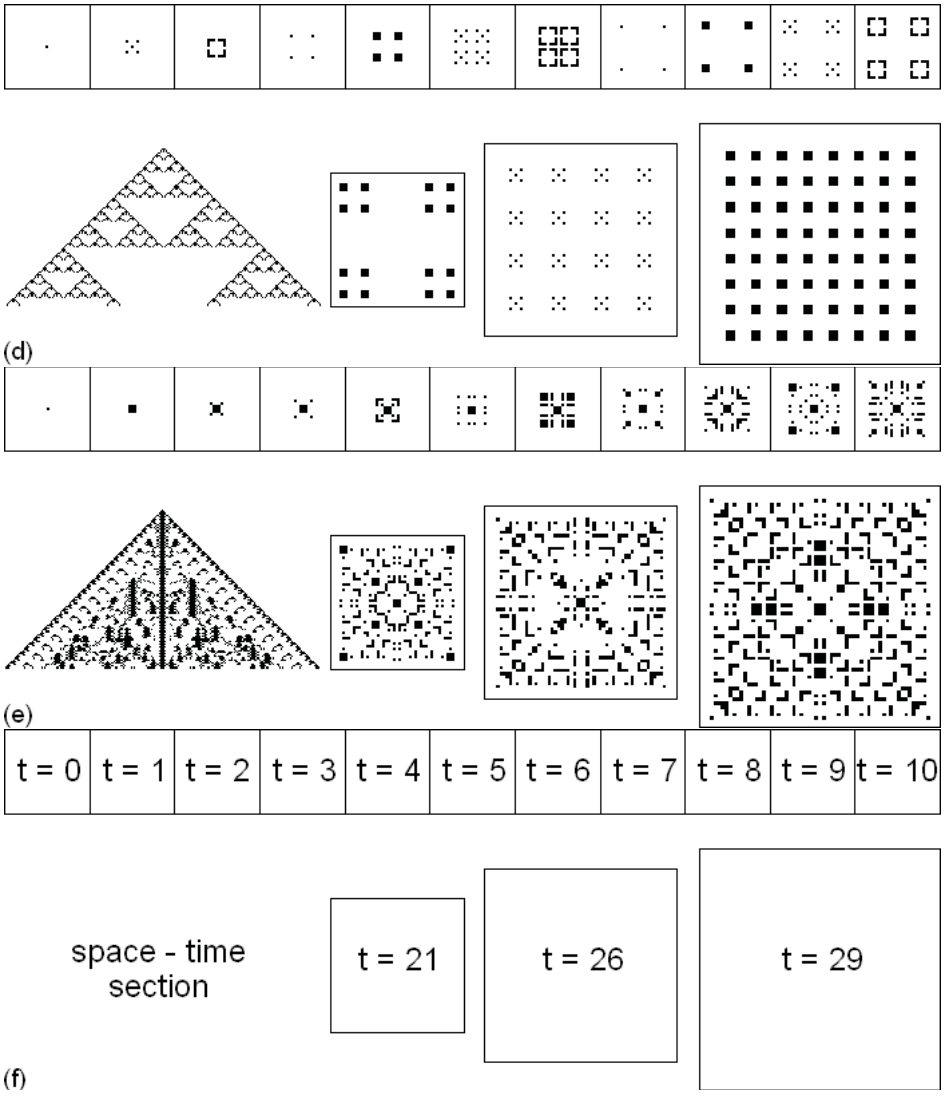

Figure 5: Typical **C**-type patterns. (a)$\mathcal{F}_{(0,1.65,1.0834,1)}$, (b)$\mathcal{F}_{(0,1.65,0.2375,1)}$, (c)$\mathcal{F}_{(0,2.6,2.52,1)}$, (d)$\mathcal{F}_{(1,0.6,2.67,0)}$, (e)$\mathcal{F}_{(1,0.6,2.4,0)}$, (f) Explanatory map of the evolving dynamics. The space-time section is the temporal projection of the square lattice's main diagonal line of cells.

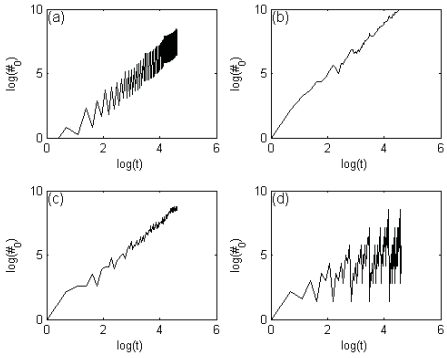

Figure 6: Growth dimensions defined as the ratio of the logarithm of black cells over the logarithm of time. The presented codes are: (a)$\mathcal{F}_{(0,1.65,1.0834,1)}$ (b)$\mathcal{F}_{(0,1.65,0.2375,1)}$ (c)$\mathcal{F}_{(1,0.6,2.4,0)}$ (d)$\mathcal{F}_{(1,0.6,2.67,0)}$.

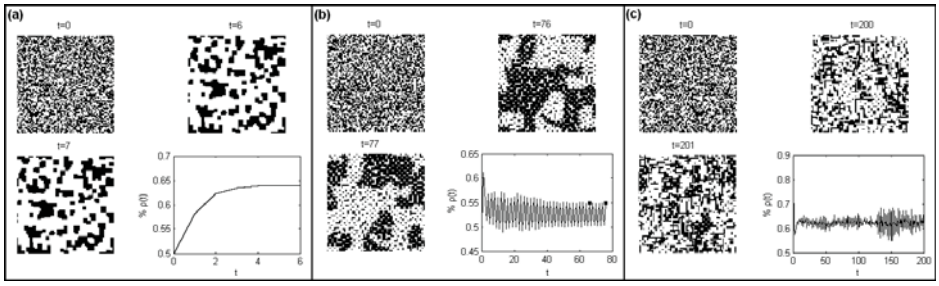

Figure 7: The $\mathcal{F}$ model starting from random seeds. (a) $\mathcal{F}_{(1,0,0,1)}$ - the system reaches a static final state. (b)$\mathcal{F}_{(0,1,1,0)}$- the system oscillates in a period-10 cycle. (c) $\mathcal{F}_{(0.5001,0.5,1,0)}$- the system behaves aperiodically.

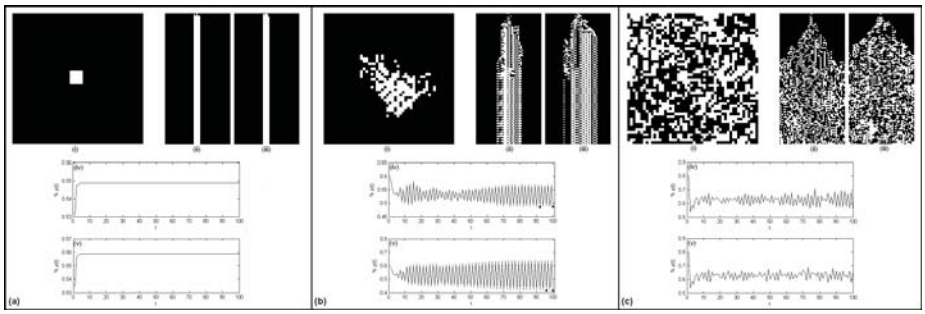

Figure 8: Difference patterns of the $\mathcal{F}$-rule starting from random seeds. (i): the difference pattern after 100 iteration. (ii),(iii): space-time sections of the horizontal and the diagonal line of the state space.(iv), (v): the $\rho(t)$ index of the resulting orbits.